Range Correlation Effect on ISM Band I/Q CMOS Radar for Non-Contact Vital Signs Sensing

Amy D. Droitcour, Olga Boric-Lubecke*, Victor M. Lubecke*, Jenshan Lin†, Gregory T. A. Kovacs
Center for Integrated Systems, Stanford University, Stanford, California, USA 94305
*Bell Laboratories, Lucent Technologies, Murray Hill, New Jersey, USA 07974
†Agere Systems, Holmdel, New Jersey, USA 07733

Abstract **– A quadrature direct conversion microwave Doppler radar has been fully integrated in 0.25 μm CMOS. This ISM band radar chip has been used to detect heart and respiration movement 50 cm from the subject. While oscillator phase noise is a performance-limiting factor in CW radar systems, the range correlation effect enables measurement of small phase modulations in spite of the notoriously high phase noise of the on-chip CMOS oscillator. This is the first reported quantitative experimental verification of the range correlation effect.**

I. INTRODUCTION

Microwave Doppler radar can be used as a non-contact, non-invasive method to measure heart and respiration rate. [1-3] This has potential in sleep apnea monitoring applications for both infants and adults. Although rates of Sudden Infant Death Syndrome (SIDS) have sharply declined in the past ten years, SIDS is still the third leading cause of infant mortality [4]. Many more infants suffer from apnea [5]. Obstructive Sleep Apnea Syndrome (OSAS) affects 4% of all adult males and has many symptoms, including hypertension, psychological distress, and cognitive impairment [6]. Doctors often prescribe chest-strap cardio-respiratory monitors for infants at high risk of SIDS and for infants and adults with symptoms of OSAS [5,7]. The Doppler radar monitor offers a non-contact alternative, which may be less intrusive.

Two challenging problems with Doppler measurement of chest wall movement are the translation of oscillator phase noise to output amplitude noise and artifacts in the signal due to motion not related to respiration or circulation. This paper addresses the phenomenon that enables measurement of heart and respiration movement with a source with as much phase jitter as an on-chip CMOS oscillator. If the same source is used for transmitting and receiving, the phase noise of the received signal is correlated with that of the local oscillator (LO), with the level of correlation dependent on the time delay between them. In a radar application, this time delay is proportional to the target range – hence, this phase noise reducing effect is known as range correlation [8]. Range correlation is particularly important in measuring chest wall movement since the heart and respiration information is encoded in phase modulations of 0.1-10Hz, where the phase noise is near its peak [3]. Due to the range correlation filtering effect, phase noise at 10Hz offset is predicted to decrease by 134dB [3,8]. This is the first reported quantitative experimental verification of the range correlation theory. The chip presented in this paper uses a quadrature receiver to avoid null points [9] and thus improve the accuracy of radars described in [2,3]. Heart and respiration rate has been detected at a 50 cm distance.

II. DOPPLER THEORY AND RANGE CORRELATION

A continuous wave (CW) radar system transmits a single tone signal, $T(t)=\cos(2\pi ft+\phi(t))$ where $\phi(t)$ is the phase noise of the oscillator. This signal is reflected from a target at a nominal distance d_0, with a time varying displacement given by $x(t)$. At the receiver, the signal is given by $R(t)$ in Eq. (1), where λ is the wavelength.

$$R(t)\approx\cos\left[2\pi ft-\frac{4\pi d_0}{\lambda}-\frac{4\pi x(t)}{\lambda}+\phi\left(t-\frac{2d_0}{c}\right)\right] \quad (1)$$

This received signal is the same as the transmitted signal with a time delay determined by the nominal distance of the target, and with its phase modulated by the periodic motion of the target. The information about the periodic target motion can be demodulated if this signal is multiplied by an LO signal that is the same as the transmitted signal. CW radar systems use the same oscillator for the transmitter and the LO.

When the received and LO signals are mixed and low pass filtered, the resulting signal is given in Eq. (2).

$$B(t)=\cos\left[\theta+\frac{4\pi x(t)}{\lambda}+\Delta\phi(t)\right] \quad (2)$$

The constant phase shift, θ, is dependent on the nominal distance to the target, d_0, and $\Delta\phi$ is the residual phase noise as given in Eq. (3).

$$\Delta\phi(t)=\phi(t)-\phi\left(t-\frac{2d_0}{c}\right) \quad (3)$$

0-7803-7695-1/03/$17.00 © 2003 IEEE

When the received signal and the LO are in quadrature and the change in displacement is small compared to the wavelength, the baseband output signal is proportional to the time varying displacement of the target. When the target is a person, the baseband output voltage is directly proportional to the chest wall movement.

The range correlation theory describes how the residual phase noise affects the noise spectrum at the IF, and it was first proposed in the early days of radar to explain why CW radar systems were not swamped by ground clutter noise [10]. More recently, an equation calculating the IF noise spectral density, $S_{\Delta\phi}(f)$, from the RF phase noise spectral density, $S_{\phi}(f)$, has been proposed. It is shown in Eq. (4), where R is the range to the target, and f is the offset frequency from the carrier [8].

$$S_{\Delta\phi}(f) = S_{\phi}(f)\left[4\sin^2\left(2\pi\frac{Rf}{c}\right)\right] \qquad (4)$$

This indicates that at a low offset frequency, the IF noise spectrum will increase proportional to the square of the target range. The IF noise spectrum will drop off as the square of the offset frequency, so the phase noise will be effectively attenuated by a filter with a slope of -20dB per decade.

III. Doppler Radio Architecture

A block diagram and a chip micrograph of the Doppler radio are shown in Fig. 1 and Fig. 2. The VCO that provides the RF_{out} and LO dissipates 25mW, with -60dBc/Hz phase noise at 10kHz offset [3]. The external source port provides the option of bypassing the on-chip VCO for testing purposes. The oscillator signal is split into the RF output signal that drives the antenna and the LO signal that is used for demodulation. The LO is amplified with a low noise amplifier (LNA) [12], and then split into two quadrature LO signals for I and Q receiver chains. The quadrature signals are created with an RC-CR circuit [13]. Another LNA amplifies each of these signals to provide I/Q isolation, and then a passive LC balun [12] transforms the single ended LO into the differential LO required by the double balanced mixer [11]. The RF input signal is split in two for I and Q channels, and active buffer amplifiers [3] provide differential RF signals to feed the mixer [12]. This chip has quadrature outputs, so phase demodulation null points, when the LO and RF signals are either in phase or 180° out of phase, can be avoided [9].

The chip was fabricated using an Agere 0.25 µm CMOS process with five metal levels. Inductor Q of 5-10 was obtained using the 3 µm thick top metal level. The chip is 4000 x 4200 μm^2, and is packaged in an Amkor TQFP exposed-pad package. The radio dissipates 180mW, and provides 3dBm RF output power at 2.3 GHz. With an external source, the chip can be used in the frequency range of 2.2 to 2.5 GHz.

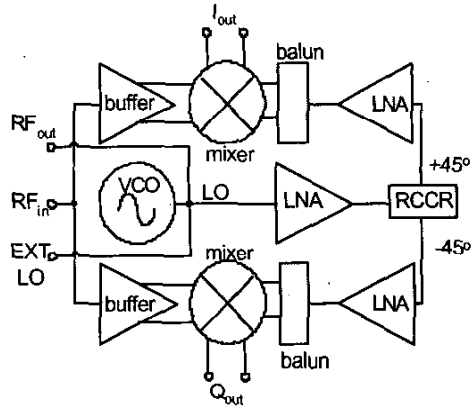

Fig. 1. Block diagram of quadrature transceiver.

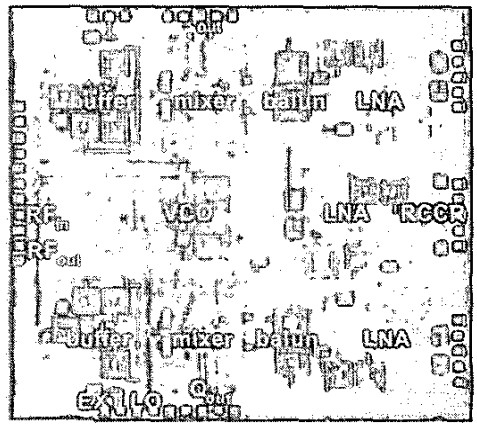

Fig. 2. Photograph of 4.2 x 4.0 mm^2 quadrature transceiver.

IV. Testing Procedure and Results

The close-in phase noise of the VCO was measured at the RF_{out} port using a HP E5500 phase noise measurement system with the FM discriminator technique and a 15-ns delay line. The phase noise spectral density is shown in Fig. 3. To avoid errors due to spurs in the phase noise measurement, a –30dB/decade line fit to the phase noise data was used to calculate the baseband noise after range correlation [Eq. (4)], which is shown for different time delays in Fig. 3. The amplitude noise of the oscillator was also measured with the HP E5500 system. It was under -

100 dBc/Hz, and therefore below the phase noise for frequencies under 10Hz, even after range correlation.

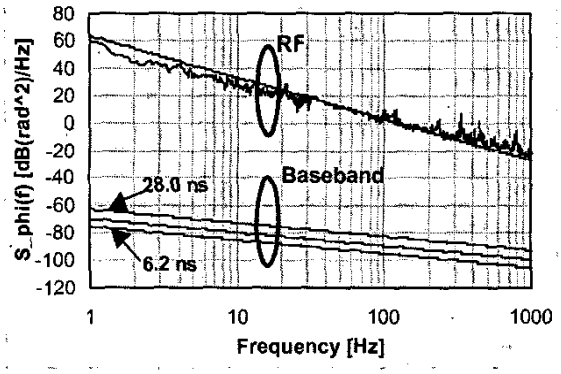

Fig. 3. Measured phase noise and –30dB/decade fit line (top traces) and predicted baseband noise for time delays of 20.8, 12.6, and 6.2 ns (bottom three traces, from top to bottom).

The range correlation theory was verified by measuring the baseband noise spectrum at I/Q output with varying delay between the transmitter and receiver. To ensure consistent measurements, the RF and LO signals were kept in quadrature so the maximum phase to voltage sensitivity is maintained. A Pasternack phase shifter (PE8442) was used to tune the phase relationship of the two signals until the DC component of the baseband signal was zero.

The RF ouput of the radar chip was connected to the phase shifter input through a 30-cm SMA cable and a 10dB attenuator to avoid any loading effects from the phase shifter. An SMA cable connected the phase shifter output to the RF input of the chip. The length of this cable was varied to change the time delay between the RF and LO signals. The baseband output of the chip was measured with a HP89410A vector signal analyzer. The baseband noise spectrum from 1 Hz to 1 kHz was measured with a 1 Hz resolution bandwidth and RMS averaged over 5 measurements. The baseband noise spectrum measurements were converted to a phase noise equivalent by calculating the ratio of the measured noise power to the power a 30 kHz IF signal would have with the same RF power. This was then converted to spectral density of phase fluctuation by multiplying by 2 [14]. The time delay, equivalent IF power, and the predicted and measured phase fluctuation spectral density at 1 Hz, 10 Hz, 100Hz, and 1 kHz for the various cable lengths are given in Table 1, and the measured phase fluctuation spectral density is plotted in Fig. 4.

The measured baseband phase noise spectral density was in the same range as predicted based on the previously measured phase noise and range correlation theory. The measured phase noise increased as the time delay increased, as was predicted. Some variation in the measurement may be due to the RF and LO signals not being exactly in quadrature and affecting the phase demodulation sensitivity. The phase noise was not measured at the same time as the range correlation measurements, and this may be another cause for some of the discrepancy between the predictions and measured results.

Time delay	[ns]	6.2	12.6	28.0
S_{phi}(1 Hz) [dB/Hz]	Predicted	-75.7	-70.1	-63.1
	Measured	-74.7	-67.3	-57.5
S_{phi}(10 Hz) [dB/Hz]	Predicted	-85.6	-80.0	-73.0
	Measured	-87.9	-82.2	-74.8
S_{phi}(100 Hz) [dB/Hz]	Predicted	-95.6	-90.0	-83.0
	Measured	-100	-98.6	-91.7
S_{phi}(1 kHz) [dB/Hz]	Predicted	-106	-100	-93.0
	Measured	-108	-105	-99.9

Table. 1. Baseband spectral density of phase fluctuation predicted with range correlation theory based on the line fit to the phase noise plot, and measured for various time delays.

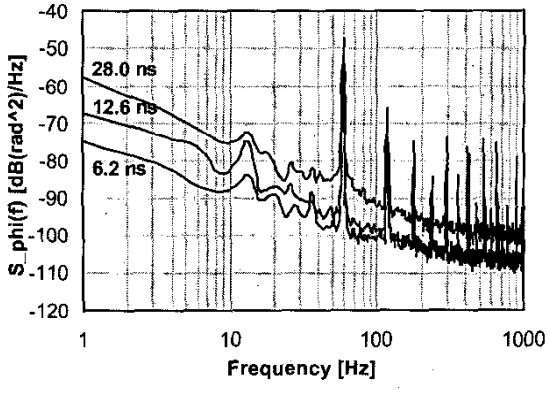

Fig. 4. Measured spectral density of phase fluctuation at baseband for time delays of 6.2, 12.6, and 28.0 ns (from bottom to top).

For the measurements of heart and respiration rate, an experimental setup similar to that in [2] and [3] was used. A single Antenna Specialists ASPPT2988 ISM band patch antenna with 60° by 80° beamwidth was used with a Mini-Circuits ZAPD-4 power splitter for all measurements. The subject was seated facing the antenna, at a distance of 50cm. A finger pressure pulse sensor (UFI-1010) provided

a reference for heart activity. The baseband output was amplified by 33 dB and filtered with programmable LNAs (SR560) to remove DC offset and avoid aliasing. The heart and respiration signals were separated with a Matlab script using techniques similar to those given in [15].

Respiration and heart traces for both outputs are shown with a wired reference in Fig. 5. In this measurement, the Q signal (second and fourth traces) is in the phase demodulation null point, and has a much smaller magnitude than the I signal (first and third traces). The heart rate is 70 beats per minute and the respiration rate is 14 breaths per minute. The heart rate measured with the radar system is within 0.5 beats per minute of the reference 81% of the time for the I trace and 70% of the time for the Q trace.

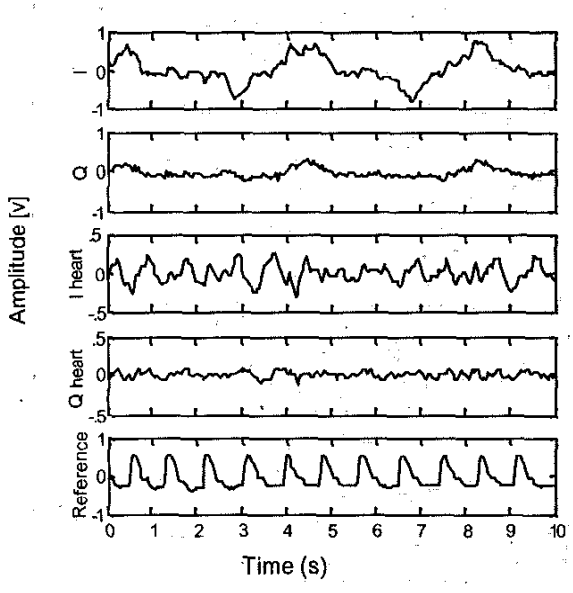

Fig. 5. Respiration and heart traces. This measurement was made 50 cm from the subject.

V. CONCLUSIONS

A fully quadrature microwave Doppler radar circuit has been integrated in low-cost silicon, and the benefit of the quadrature architecture in eliminating null points has been demonstrated. The range correlation effect reduces the close-in phase noise of the CMOS oscillator sufficiently to enable the remote detection of heart and respiration movement. This is the first published verification of the range correlation effect. With more advanced signal processing and better system integration, this chip could be used in a monitor for SIDS and OSAS. A prototype monitoring device, based on this chip, is currently being developed for these applications.

ACKNOWLEDGEMENTS

The authors thank Carsten Metz and Merv Budge for helpful discussions and Agere Systems for chip fabrication. The authors acknowledge financial support from NASA Ames Research Center and from Lucent Technologies through the GRPW fellowship. M. Zeirdt's assistance with board assembly and F.P. Hrycenko's and T. Gabara's support in chip layout are greatly appreciated.

REFERENCES

[1] J.C. Lin, "Microwave Sensing of Physiological Movement and Volume Change: A Review," *Bioelectromagnetics*, vol. 13, pp.557-565, 1992.

[2] A.D. Droitcour, et al., "A Microwave Radio for Doppler Radar Sensing of Vital Signs," *2001 MTT-S IMS Digest*, vol.1 pp.175-178, 2001.

[3] A.D. Droitcour, et al., "0.25 μm CMOS and BiCMOS Single-chip Direct-conversion Doppler Radars for Remote Sensing of Vital Signs," *2002 ISSCC Digest*, vol.1 pp.348-348, 2002.

[4] D.L. Hoyert, et al. "Annual Summary of Vital Statistics: 2000," *Pediatrics*, vol. 108, no. 6, 2001.

[5] "Infantile Apnea and Home Monitoring", *NIH Consensus Statement* vol. 6, no. 6, September, 1986.

[6] A.N. Vgontzas, A. Kales, "Sleep and Its Disorders," *Ann. Rev. Medicine*, vol. 50, pp.387-400, 1999.

[7] R. Ferber et al., "Portable Recording in the Assessment of Obstructive Sleep Apnea," *Sleep*, vol. 17, pp. 378-392, 1994.

[8] M.C. Budge, Jr. and M.P. Burt, "Range Correlation Effects on Phase and Amplitude Noise," *Proceedings of IEEE Southeastcon*, 1993.

[9] J. Seals, S.R. Crowgey, S.M. Sharpe, "Electromagnetic Vital Signs Monitor" Atlanta: Georgia Tech Res. Inst. Biomed Div., 1986.

[10] R.S. Raven, "Requirements on Master Oscillators for Coherent Radar," *Proc. IEEE*, vol. 54, no. 2, 1966.

[11] P. Gould et al., "CMOS Resistive Ring Mixer for GSM 900 and DCS 1800 Base Station Applications," *2000 MTT-S IMS Digest*, vol. 1, pp.521-524, 2000.

[12] O. Boric-Lubecke, et al., "DCS1800 Receiver Integrated in 0.25 μm CMOS," *2002 MTT-S IMS Digest*, vol. 2, pp.1049-1052, 2002.

[13] B. Razavi, *RF Microelectronics*, New York: Prentice Hall, 1997.

[14] G.D. Vendelin, et al., *Microwave Circuit Design Using Linear and Nonlinear Techniques*, New York: Wiley, 1990.

[15] B. Lohman, et al., "A Digital Signal Processor for Doppler Radar Sensing of Vital Signs," *Proc. 23rd Ann. Conf. IEEE EMBS*, vol. 4, pp. 3359-3362, 2001.